

## Microporous Materials

**High H<sub>2</sub> Adsorption in a Microporous Metal–Organic Framework with Open Metal Sites\*\***

Banglin Chen,\* Nathan W. Ockwig,  
Andrew R. Millward, Damacio S. Contreras, and  
Omar M. Yaghi\*

Metal–organic frameworks (MOFs) are a rapidly growing class of porous materials that are studied for their amenability to design<sup>[1]</sup> and extraordinary permanent porosity.<sup>[2]</sup> The recent discovery that MOFs take up significant amounts of

[\*] Prof. B. Chen, D. S. Contreras

Department of Chemistry  
University of Texas–Pan American  
Edinburg, TX 78541-2999 (USA)  
Fax: (+1) 956-384-5006  
E-mail: banglin@utpa.edu

N. W. Ockwig, A. R. Millward, Prof. O. M. Yaghi  
Materials Design and Discovery Group  
Department of Chemistry  
University of Michigan  
Ann Arbor, MI 48109-1055 (USA)  
Fax: (+1) 734-615-9751  
E-mail: oyaghi@umich.edu

[\*\*] This work was supported by the University of Texas–Pan American through a start-up fund and a Faculty Research Council award to B. Chen, and, in part, by a Welch Foundation grant (BG-0017) to the Department of Chemistry at UTPA, a grant from the National Science Foundation to O.M.Y. (DMR-0242630), and the Department of Energy (O.M.Y.).



Supporting information for this article is available on the WWW under <http://www.angewandte.org> or from the author.

hydrogen has further intensified research in this area.<sup>[3]</sup> In particular, the focus remains on identifying strategies for designing MOFs with high hydrogen-storage capacities. We have already found that both the metal-oxide units and the organic links are important features for hydrogen binding,<sup>[3a,d]</sup> and that interpenetrating MOFs take up more hydrogen than their noninterpenetrating counterparts.<sup>[3d]</sup> In this report, we highlight the synthesis and structure of a MOF (named MOF-505) based on the NbO topology which has two kinds of pores, open metal sites, permanent porosity, and a high capacity for hydrogen adsorption.

We have previously synthesized MOFs with  $\text{Cu}_2(\text{CO}_2)_4$  “paddle-wheel” units, and illustrated their use in the design of 0-periodic discrete<sup>[4]</sup> and 3-periodic extended structures.<sup>[5,10]</sup> MOF-505 was synthesized under analogous conditions: the solvothermal reaction of 3,3',5,5'-biphenyltetracarboxylic acid ( $\text{H}_4\text{bptc}$ ; 25 mg, 0.076 mmol)<sup>[6]</sup> and  $\text{Cu}(\text{NO}_3)_2 \cdot (\text{H}_2\text{O})_{2.5}$  (52 mg, 0.22 mmol) in *N,N*-dimethylformamide (DMF)/ethanol/ $\text{H}_2\text{O}$  (3:3:2 v/v/v) at 65 °C for 24 h gave green, block-shaped crystals (47 mg, 86% yield based on  $\text{H}_4\text{bptc}$ ). The compound was formulated as  $[\text{Cu}_2(\text{bptc})(\text{H}_2\text{O})_2(\text{dmf})_3(\text{H}_2\text{O})]$  by elemental microanalysis<sup>[7]</sup> and single-crystal X-ray diffraction studies.<sup>[8]</sup>

The  $\text{Cu}_2(\text{CO}_2)_4$  unit is a square secondary building unit (SBU; Figure 1 A) that is defined by the carboxylate carbon atoms, and the  $\text{bptc}^{4-}$  unit is a rectangular SBU that is defined by the 3, 3', 5, and 5' carbon atoms (Figure 1 B). The carboxylate functionalities of the  $\text{bptc}^{4-}$  ligand are nearly coplanar with the biphenyl rings (the dihedral angle between the carboxylate group and the phenyl ring is 7.4°).<sup>[2]</sup> Thus, when the square SBUs are linked to the biphenyl rings, they must be mutually orthogonal (Figure 1 C), an aspect that is the hallmark of the NbO topology.<sup>[9,10]</sup> The crystal structure of MOF-505 (Figures 1 D and E) clearly shows that the link has predisposed the inorganic square SBUs at nearly 90° angles (94.4°) to the organic rectangular SBUs. This arrangement yields an overall 3-periodic network which has two kinds of pores. The first of these pores is defined by six inorganic SBUs (representing the faces of a cubic NbO subunit) with a spherical volume of 290 Å<sup>3</sup> and a pore diameter of 8.30 Å (Figures 1 D and F), while the second, and larger, pore is defined by six organic SBUs (again representing the faces of a cubic NbO subunit) and has a solvent-accessible void of 540 Å<sup>3</sup> with a pore diameter of 10.10 Å (Figures 1 E and G).<sup>[11]</sup> These roughly spherical pores are arranged in a rhombohedrally distorted CsCl-type fashion with the small pores surrounded by eight large pores, each of which is also surrounded by eight small pores. There are a total of six pores (three large and three small) per unit cell, which are coupled through an interconnected porous network of 6.70 Å diameter apertures. This provides a total accessible free volume of 2713 Å<sup>3</sup> (37.1 %).<sup>[11,12]</sup>

Thermal gravimetric analysis (TGA) and powder X-ray diffraction (PXRD) patterns were used to evaluate the framework stability under solvent-exchange conditions. PXRD reveals the same pattern of intense diffraction lines in each of the simulated, as-synthesized, and acetone-exchanged materials (see Supporting Information). However, upon desolvation of the exchanged material, decreased

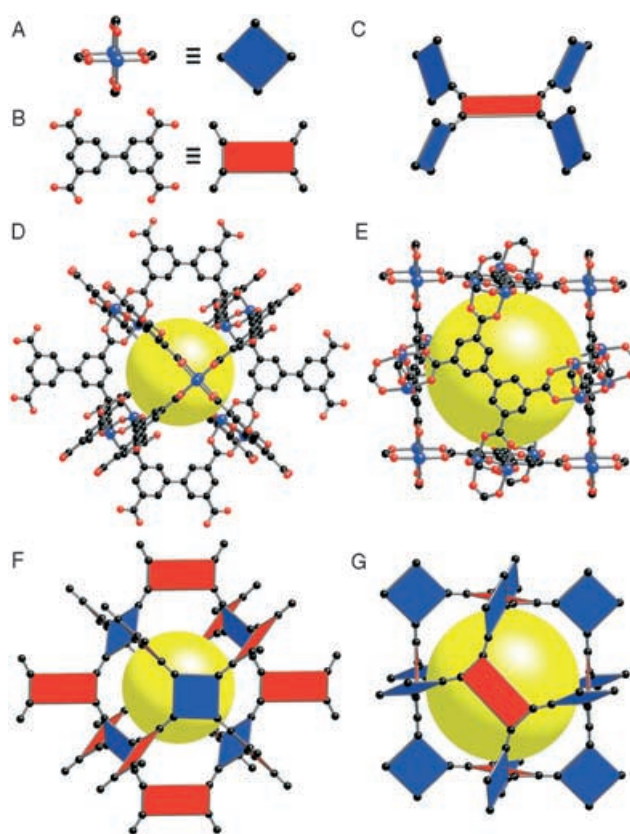


**Figure 1.** The single-crystal X-ray structure of MOF-505 showing A)  $\text{Cu}_2(\text{CO}_2)_4$  units (blue, square SBUs) and B)  $\text{bptc}^{4-}$  units (red, rectangular SBUs) that are C) orthogonally joined. The overall 3-periodic crystal structure (D, E; Cu blue, C black, O red, and the yellow sphere represents the largest sphere that would occupy the cavity without contacting the interior van der Waals surface) has two different types of pores and an underlying NbO-type net (F, G). Hydrogen atoms, guest molecules, and terminal solvent molecules have been omitted for clarity.

diffraction intensities and broadened reflections were observed in the PXRD pattern. This indicates some loss of long-range order but not necessarily loss of porosity, as detailed below. To examine the thermal stability of MOF-505 and estimate the temperature of desolvation we conducted a TGA study: the weight loss of 30.83 % below 250 °C corresponds to the liberation of 2.5 acetone molecules and three water molecules per  $\text{Cu}_2\text{bptc}$  formula unit (calcd: 30.53 %).

To evaluate whether the framework structure is maintained upon evacuation of the pores, we obtained the gas sorption isotherms using a Cahn C-1000 microgravimetric balance to measure the change in mass of samples suspended within a glass enclosure under a chosen gas atmosphere. The as-synthesized MOF-505 crystalline sample was activated by immersion in acetone for 72 h (3 × 50 mL for 24 h each) to exchange the dmf guests. The resulting damp, blue-green solid (617 mg) was loaded into the apparatus and evacuated (<10<sup>−3</sup> Torr) in three stages (I–III), with both weight loss and color changes being recorded (stage I: 15 h at room temperature (weight decreased to 358 mg, 42.0 % weight loss, light blue); stage II: heating at 70 °C for 15 h (weight

decreased to 325 mg, 5.3% weight loss, dark blue); and stage III: a final dehydration at 120 °C for 12 h (weight decreased to 296 mg, 4.7% weight loss, purple)), to leave the evacuated sample. Nitrogen and hydrogen isotherms were obtained at each of these activation stages (I–III) as elaborated below. To ensure complete removal of all volatile contaminants from the system, the gas manifold was evacuated overnight and heated to 100 °C prior to the introduction of gas. The system was purged three times at room temperature with the gas to be studied (ultra-high-purity grade, 99.999%) before cooling to 77 K with liquid nitrogen. The sample temperature was monitored by a thermocouple suspended in close proximity to the sample. Pressures were measured with two MKS Baratron 622 A pressure transducers (10 and 1000 Torr, accuracy  $\pm 0.25\%$  of range). The gas was introduced incrementally and data points were recorded when no further change in mass was observed ( $< 0.02$  mg per 10 min). An empirical buoyancy correction was applied to all data points based on the buoyancy experienced

activated material obtained after stage III shows a substantial increase in the sorption to give a final  $N_2$  uptake of  $526 \text{ mg g}^{-1}$  ( $A_s = 1830 \text{ m}^2 \text{ g}^{-1}$ ,  $K_{N_2} = 0.362$ , and  $V_p = 0.63 \text{ cm}^3 \text{ g}^{-1}$ ). These data are summarized in Table 1.

**Table 1:** Sorption data for MOF-505.

Activation Stage	$T$ [°C]	Uptake [ $\text{mg g}^{-1}$ ] $N_2$ $H_2$	$A_s$ [ $\text{m}^2 \text{ g}^{-1}$ ] <sup>[a]</sup>	$K_{N_2}$ [ $\text{Torr}^{-1}$ ] <sup>[a,c]</sup>	$K_{H_2}$ [ $\text{Torr}^{-1}$ ] <sup>[a,d]</sup>	$V_p$ [ $\text{cm}^3 \text{ g}^{-1}$ ] <sup>[b]</sup>
I	25	278      14.1	967	0.193	0.0071	0.33
II	70	386      19.7	1343	0.327	0.0070	0.45
III	120	526      24.7	1830	0.362	0.0086	0.63

[a] Calculated from a Langmuir fit of the data. [b] Calculated by extrapolation of the Dubinin–Radushkevich equation. [c] Calculated from  $N_2$  data. [d] Calculated from  $H_2$  data.

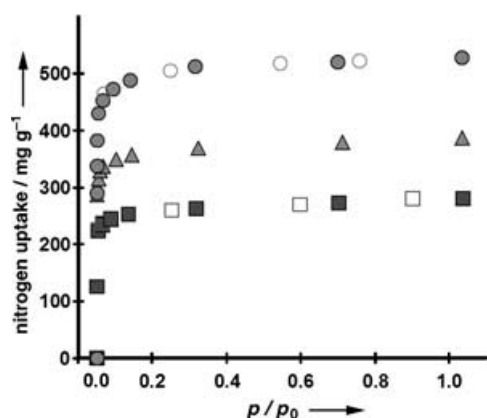


**Figure 2.**  $N_2$  isotherms for MOF-505 (77 K) after three different activation stages: stage I (25 °C, squares), stage II (70 °C, triangles), and stage III (120 °C, circles); filled shapes indicate adsorption and open shapes indicate desorption data points.

by standard aluminum foil weights within the pressure range of the gas at 77 K.

Nitrogen sorption by this material clearly shows reversible type-I isotherms at each of the activation stages (Figure 2), indicative of permanent porosity. At stage I (25 °C), an uptake of  $278 \text{ mg g}^{-1}$  is achieved, with an equivalent Langmuir surface area ( $A_s$ ) of  $967 \text{ m}^2 \text{ g}^{-1}$ , and  $K_{N_2} = 0.193$  for a  $16.2 \text{ \AA}^2$  molecular cross-section. Assuming liquid-nitrogen density ( $0.808 \text{ g cm}^{-3}$ ) in the pores, extrapolation of the Dubinin–Radushkevich equation<sup>[13]</sup> from the low-pressure data points yields an available micropore volume ( $V_p$ ) of  $0.33 \text{ cm}^3 \text{ g}^{-1}$ . Further evacuation of the pores (stage II) removes an additional 5.3% of guests, providing a 36% greater uptake ( $386 \text{ mg g}^{-1}$ ,  $A_s = 1343 \text{ m}^2 \text{ g}^{-1}$ ,  $K_{N_2} = 0.327$ , and  $V_p = 0.45 \text{ cm}^3 \text{ g}^{-1}$ ) than that observed in the first stage. The fully

The hydrogen isotherms of MOF-505 measured at 77 K at the same stages of activation are shown in Figure 3. This temperature is well above the critical temperature (33 K) for

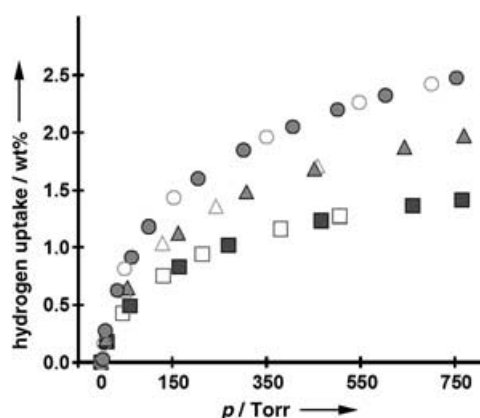


**Figure 3.**  $H_2$  isotherms for MOF-505 (77 K) after three different activation stages: stage I (25 °C, squares), stage II (70 °C, triangles), and stage III (120 °C, circles); filled shapes indicate adsorption and open shapes indicate desorption data points.

hydrogen,<sup>[14]</sup> which suggests that condensation in the pores would be unlikely and complete saturation would not be achieved without much higher pressures. The isotherms measured (0 to 750 Torr) did not show saturation; however, the maximum uptake at 750 Torr for each of the three hydrogen isotherms demonstrates similar increases in capacity to those observed in the nitrogen isotherms, with the fully activated MOF-505 adsorbing an exceptional 2.47 wt% hydrogen at 750 Torr and 77 K. This extraordinary hydrogen sorption capacity is unprecedented in previously reported MOF materials under these conditions.<sup>[3b]</sup>

Removal of noncoordinated guests during activation has at least two positive effects on the adsorption capacity: a decrease of sample mass and an increase of available micropore volume and specific surface area. However, removal of the water ligands (bound axially to the copper centers) has the same benefits and also introduces open metal sites that we think enhance the hydrogen–framework interaction. The existence of such open metal sites in MOFs has been confirmed previously by single-crystal X-ray diffraction of

MOF-11.<sup>[5b]</sup> Room temperature evacuation overnight (stage I) yields an initial hydrogen uptake of  $14.1 \text{ mg g}^{-1}$  ( $1.41 \text{ wt } \% \text{ H}_2$ ; Table 1). The second activation step (stage II) removes an additional  $5.3 \text{ wt } \%$  (partial dehydration) and increases the hydrogen uptake by  $5.6 \text{ mg g}^{-1}$  ( $19.7 \text{ mg g}^{-1}$ ,  $1.97 \text{ wt } \% \text{ H}_2$ ). Further removal of  $4.7 \text{ wt } \%$  (stage III, complete dehydration) increases the hydrogen uptake capacity by an additional  $5.0 \text{ mg g}^{-1}$  to  $24.7 \text{ mg g}^{-1}$  or  $2.47 \text{ wt } \% \text{ H}_2$ . Upon comparison, the initial activation step (stage I, evacuation of bulk guests) shows an increase in hydrogen sorption of  $0.34 \text{ mg g}^{-1}$  per percent mass loss whereas the last two activation steps (stages II and III, dehydration with loss of six water molecules per  $\text{Cu}_2\text{bptc}$  formula unit) show a corresponding increase of  $1.06 \text{ mg g}^{-1}$  per percent mass loss during activation. Indeed, at stage I the  $\text{H}_2$  uptake ( $77 \text{ K}$ ) is  $14.1 \text{ mg g}^{-1}$ , while the fully activated material (stage III) containing open metal sites displays an uptake nearly twice as high ( $24.7 \text{ mg g}^{-1}$ ) despite only a  $10 \text{ } \%$  mass loss. The lack of any hysteresis in the isotherm illustrates that this physisorption process is completely reversible, and that the presence of these open metal sites does not hamper the desorption process, nor do the pore apertures of  $6.70 \text{ \AA}$  significantly hinder small-molecule diffusion through the host framework. Although there are slight curvatures in the Langmuir plots (leading to some degree of uncertainty) some insight pertinent to this specific system can still be gleaned. Increasing  $K_{\text{H}_2}$  values reveal a trend toward increasing hydrogen affinity of the fully dehydrated framework relative to the partially evacuated material (Table 1).

Although we speculate that the open metal sites have a favorable impact on the hydrogen sorption capacity of MOF-505, further experimentation is required to verify this. Another plausible explanation for the high hydrogen uptake capacity of MOF-505 is a simple correlation between specific surface area ( $A_s$ ) and uptake. Similar correlations have been made for activated carbons and zeolites<sup>[15]</sup> but have yet to be established for MOF materials. In fact, we would like to specifically point out that, so far, MOF materials with very high surface areas ( $1000\text{--}4500 \text{ m}^2 \text{ g}^{-1}$ ) do not cleanly follow this correlation.<sup>[3d]</sup> Nevertheless, we do observe that each stage of activation is accompanied by distinct changes in sample color, which is consistent with a change in the coordination environment of the metal sites as a result of the removal of terminal ligands. As-synthesized MOF-505 is blue-green and the first-stage activation changes this to light blue; further activation deepens the blue color, while the final activation step yields a deep-purple material. An activated sample exposed to ambient air for  $36 \text{ h}$  shows a dramatic color change from purple back to blue-green, with the subsequent TGA showing a loss of  $18.7 \text{ wt } \%$  below  $250^\circ\text{C}$ , corresponding to the loss of six water molecules per  $\text{Cu}_2\text{bptc}$  formula unit (calcd:  $19.3 \text{ } \%$ ). Undoubtedly, two of these water molecules are axially coordinated to the paddle wheels, while the remaining four may be located in the equatorial quadrants defined by adjacent carboxylate groups of every paddle wheel.

At present, we are targeting the application of MOFs to gas sorption and selective separations in order to establish their optimal performance and to establish principles for

improved inert-gas storage capacities. The unprecedented  $2.47 \text{ wt } \% \text{ H}_2$  uptake of MOF-505 is an important milestone toward achieving these objectives.

Received: December 2, 2004

Revised: March 24, 2005

Published online: May 27, 2005

**Keywords:** adsorption · copper · hydrogen · metal–organic frameworks · microporous materials

- [1] a) O. M. Yaghi, M. O'Keeffe, N. W. Ockwig, H. K. Chae, M. Eddaoudi, J. Kim, *Nature* **2003**, *423*, 705–714; b) N. W. Ockwig, O. Delgado-Friedrichs, M. O'Keeffe, O. M. Yaghi, *Acc. Chem. Res.* **2005**, *38*, 176–182; c) C. Mellot-Draznieks, J. Dutour, G. Férey, *Angew. Chem.* **2004**, *116*, 6450–6456; *Angew. Chem. Int. Ed.* **2004**, *43*, 6290–6296.
- [2] a) H. Li, M. Eddaoudi, M. O'Keeffe, O. M. Yaghi, *Nature* **1999**, *402*, 276–279; b) H. K. Chae, D. Y. Siberio-Pérez, J. Kim, Y. Go, M. Eddaoudi, A. J. Matzger, M. O'Keeffe, O. M. Yaghi, *Nature* **2004**, *427*, 523–527; c) H. Li, M. Eddaoudi, T. L. Groy, O. M. Yaghi, *J. Am. Chem. Soc.* **1998**, *120*, 8571–8572; d) G. Férey, C. Serre, C. Mellot-Draznieks, F. Millange, S. Surble, J. Dutour, I. Margiolaki, *Angew. Chem.* **2004**, *116*, 6456–6461; *Angew. Chem. Int. Ed.* **2004**, *43*, 6296–6301; e) R. Kitaura, K. Seki, G. Akiyama, S. Kitagawa, *Angew. Chem.* **2003**, *115*, 444–447; *Angew. Chem. Int. Ed.* **2003**, *42*, 428–431; f) X. Zhao, B. Xiao, A. J. Fletcher, K. M. Thomas, D. Bradshaw, M. J. Rosseinsky, *Science* **2004**, *306*, 1012–1015.
- [3] a) N. L. Rosi, J. Eckert, M. Eddaoudi, D. T. Vodak, J. Kim, M. O'Keeffe, O. M. Yaghi, *Science* **2003**, *300*, 1127–1129; b) D. N. Dybste, H. Chun, S. H. Yoon, D. Kim, K. Kim, *J. Am. Chem. Soc.* **2003**, *125*, 32–33; c) G. Férey, M. Latroche, C. Serre, F. Millange, T. Loiseau, A. Percheron-Guegan, *Chem. Commun.* **2003**, 2976–2977; d) J. L. C. Rowsell, A. R. Millward, K. S. Park, O. M. Yaghi, *J. Am. Chem. Soc.* **2004**, *126*, 5666–5667; e) D. N. Dybste, H. Chun, K. Kim, *Angew. Chem.* **2004**, *116*, 5143–5146; *Angew. Chem. Int. Ed.* **2004**, *43*, 5033–5036; f) E. Y. Lee, M. P. Suh, *Angew. Chem.* **2004**, *116*, 2858–2861; *Angew. Chem. Int. Ed.* **2004**, *43*, 2798–2801; g) L. Pan, M. B. Sander, X. Huang, J. Li, M. Smith, E. Bittner, B. Bockrath, J. K. Johnson, *J. Am. Chem. Soc.* **2004**, *126*, 1308–1309; h) J. L. C. Rowsell, O. M. Yaghi, *Angew. Chem.* **2005**, *117*, accepted; *Angew. Chem. Int. Ed.* **2005**, *44*, accepted.
- [4] M. Eddaoudi, J. Kim, J. B. Wachter, H. K. Chae, M. O'Keeffe, O. M. Yaghi, *J. Am. Chem. Soc.* **2001**, *123*, 4368–4369.
- [5] a) M. Eddaoudi, D. B. Moler, H. Li, B. Chen, T. M. Reineke, M. O'Keeffe, O. M. Yaghi, *Acc. Chem. Res.* **2001**, *34*, 319–330; b) B. Chen, M. Eddaoudi, T. M. Reineke, J. W. Kampf, M. O'Keeffe, O. M. Yaghi, *J. Am. Chem. Soc.* **2000**, *122*, 11559–11560; c) B. Chen, M. Eddaoudi, S. T. Hyde, M. O'Keeffe, O. M. Yaghi, *Science* **2001**, *291*, 1021–1023.
- [6]  $\text{H}_2\text{bptc}$  was prepared according to published methods: S. J. Coles, R. Holmes, M. B. Hursthouse, D. J. Price, *Acta Crystallogr. Sect. E* **2002**, *58*, o626.
- [7] Elemental analysis (%) for MOF-505 ( $\text{C}_{25}\text{H}_{33}\text{Cu}_2\text{N}_3\text{O}_{14}$ ): calcd: C 41.32, H 4.54, Cu 17.49, N 5.78; found: C 41.09, H 4.35, Cu 17.20, N 5.61.
- [8] X-ray crystallographic data:  $\varphi$  and  $\omega$  scans were performed on a Bruker SMART APEX CCD area detector with graphite-monochromated  $\text{MoK}_\alpha$  radiation ( $\lambda = 0.71073 \text{ \AA}$ ). SAINT was used for data integration, SADABS for absorption correction, and XPREF for correction of Lorentz and polarization effects. Structure solution was performed by direct methods and subsequent difference Fourier techniques using the SHELX-



TL software suite. Data collection for a green, block-shaped crystal of MOF-505 ( $0.06 \times 0.06 \times 0.04 \text{ mm}^3$ ) was performed at  $-120^\circ\text{C}$ ; rhombohedral space group  $R\bar{3}m$  (no. 166) with  $a = 18.4826(8)$ ,  $c = 24.713(2) \text{ \AA}$ ,  $V = 7311.2(7) \text{ \AA}^3$ ,  $Z = 18$ ,  $\rho_{\text{calcd}} = 0.992 \text{ g cm}^{-3}$ ,  $\mu(\text{Mo}_{\text{K}\alpha}) = 1.338 \text{ mm}^{-1}$ ,  $F(000) = 2160$ ; a total of 10057 reflections (2072 unique,  $R_{\text{int}} = 0.0488$ ) within  $2\theta_{\text{max}} = 55.16^\circ$ ,  $T_{\text{max}} = 0.9484$ ,  $T_{\text{min}} = 0.9240$ . All non-hydrogen atoms of the extended structure, except for solvent molecules, were refined anisotropically. Electron-density contributions from diffuse scattering and disordered guest molecules were handled using the SQUEEZE procedure from the PLATON software suite. Hydrogen atoms were generated with idealized geometries. The final full-matrix least-squares refinement (based on 2072 observed reflections) on  $F^2$  converged to  $R1$  ( $I > 2\sigma(I)$ ) = 0.0361 and  $wR2$  (all data) = 0.0896 with GOF = 0.945. The maximum and minimum peaks on the final difference Fourier map corresponded to 0.549 and  $-0.269 \text{ e}^- \text{ \AA}^{-3}$ , respectively. CCDC 257470 contains the supplementary crystallographic data for this paper. These data can be obtained free of charge from the Cambridge Crystallographic Data Centre via [www.ccdc.cam.ac.uk/data\\_request/cif](http://www.ccdc.cam.ac.uk/data_request/cif).

- [9] M. Eddaoudi, J. Kim, D. Vodak, A. Sudik, J. Watcher, M. O'Keeffe, O. M. Yaghi, *Proc. Natl. Acad. Sci. USA* **2002**, *99*, 4900–4904.
- [10] M. Eddaoudi, J. Kim, M. O'Keeffe, O. M. Yaghi, *J. Am. Chem. Soc.* **2001**, *124*, 376–377.
- [11] The van der Waals radii of C (1.70 Å) and Cu (1.43 Å) were employed in the determination of distance parameters: A. Bondi, *J. Phys. Chem.* **1964**, *68*, 441–451.
- [12] As calculated using the accessible free volume method in Cerius<sup>2</sup> 4.2 from Accelrys with a probe radius of 1.45 Å.
- [13] F. Rouquerol, J. Rouquerol, K. Sing, *Absorption by Porous Solids*, Academic Press, London, **1999**.
- [14] R. C. Reid, J. M. Prausnitz, B. E. Poling, *The Properties of Gases and Liquids*, 4th ed., McGraw-Hill, New York, **1987**.
- [15] M. G. Nijkamp, J. E. M. J. Raaymakers, A. J. van Dillen, K. P. de Jong, *Appl. Phys. A* **2001**, *72*, 619–623.